

**I** Transcripts with  $R_{ss}^{H/N} < 2x, > 0.5x$

	$\kappa$	95% CI (lower, upper)	
$R_{ss}^{H/N}, pS^{H/N}$	0.16	0.08	0.24
$R_{ss}^{H/N}, T_e^{H/N}$	0.05	0.04	0.06
$T_e^{H/N}, pS^{H/N}$	0.61	0.54	0.67

All transcripts, rlog transformed  $R_{ss}$

	$\rho$
$\rho$	0.9973
95% CI	0.9972 (lower) 0.9974 (upper)
$R^2$	0.9946
p value	$< 2.2E-16$

All transcripts, rlog transformed  $R_{ss}$

	$\kappa$	95% CI (lower, upper)	
$R_{ss}^{H/N}, pS^{H/N}$	-0.01	-0.16	0.14
$R_{ss}^{H/N}, T_e^{H/N}$	0.08	0.07	0.10
$T_e^{H/N}, pS^{H/N}$	0.63	0.57	0.67

**Figure S1. Related to Figure 1.** (A) 46505 and 44974 transcripts were identified by RNA-Seq of MO and P fractions in normoxic (left panel) and hypoxic (right panel) U87MG, respectively. Relative mRNA abundance was calculated based on total read count of all sequenced fractions. Y-axis: number of transcripts; x-axis: read count (increasing from left from right). (B) Representative polysome profile of normoxic and hypoxic U87MG. Monosome (fractions 2 and 3) and polysome (fractions 7 to 10) fractions were pooled and subjected to RNA-Seq analysis. (C) Transcription intensities in normoxic and hypoxic U87MG were measured using 5-FU incorporation (1 mM final concentration). RNA polymerase I activity was specifically inhibited by Act. D (final concentration 0.04  $\mu\text{g/ml}$ ). Pan RNA polymerase activity was inhibited by Act. D (final concentration 1  $\mu\text{g/ml}$ ). 5-FU incorporation was detected by immunofluorescence (green). DNA/nuclei were stained with Hoechst (inset, blue). White scale bars represent 10  $\mu\text{m}$ . (D) Plots of  $R_{ss}$  in hypoxic ( $R_{ss}^H$ ) versus normoxic ( $R_{ss}^N$ ) U87MG based on monosome versus polysome RNA-seq analysis (Figure S1B). Plots representing all detected transcripts (left panel) and transcripts with  $R_{ss}^H/R_{ss}^N$  ( $R_{ss}^{H/N}$ ) ratios between  $<2x$  and  $>0.5x$  (right panel, black). Transcripts with  $R_{ss} < 1$  were excluded from analysis. (E) Relative abundance of pSILAC ( $pS$ )-identified proteins in hypoxic ( $pS^H$ ) versus normoxic ( $pS^N$ ) U87MG. Proteins are categorized according to the ratio of  $pS^H$  to  $pS^N$  ( $pSILAC^{H/N}$ ). (F) Plots of  $pS^H$  against  $pS^N$  for all detected transcripts (left panel) and transcripts with  $R_{ss}^H / R_{ss}^N$  ( $R_{ss}^{H/N}$ ) ratios between  $<2x$  and  $>0.5x$  (right panel). Canonical hypoxia-inducible genes are highlighted in green. Proteins detected only in normoxic or hypoxic U87MG were imputed using a truncated normal distribution with estimated mean and standard deviation from the data. Upper bound of truncated normal distribution is set to the minimum value of the observed measurements. Multiple (10,000) imputations were performed to obtain the Pearson correlation coefficient and 95% confidence interval. (G) Plots of  $T_e$  in hypoxic ( $T_e^H$ ) versus normoxic ( $T_e^N$ ) U87MG based on monosome versus polysome RNA-seq analysis (Figure S1B). Plots representing all detected transcripts (left panel), and transcripts with  $R_{ss}^{H/N}$  ratios between  $<2x$  and  $>0.5x$  (right panel). (H) Plots of  $R_{ss}$  in normoxic (top left panel) and hypoxic (top right panel) U87MG, and plots of  $T_e$  in normoxic (bottom left panel) and hypoxic (bottom right panel) U87MG. Transcripts are represented on the x-axis, arranged from lowest (left) to highest abundance (right) (Tables S1 and S2). (I) Concordance analysis between  $R_{ss}^{H/N}$ ,  $pS^{H/N}$  and  $T_e^{H/N}$  of transcripts with  $R_{ss}^{H/N}$  ratios between  $<2x$  and  $>0.5x$  (top panel), and for all transcripts following a regularized log (rlog) transformation of  $R_{ss}$  (bottom panel). Correlation analysis of rlog transformed  $R_{ss}^H$  versus rlog transformed  $R_{ss}^N$  (middle panel).

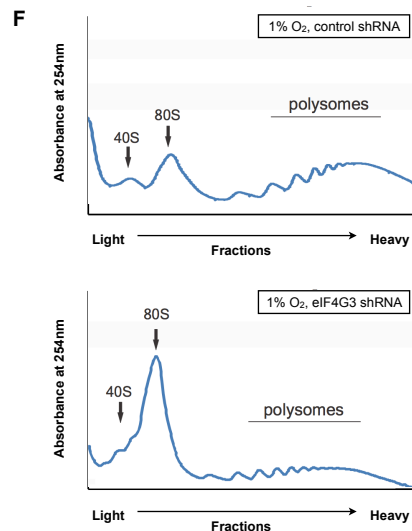
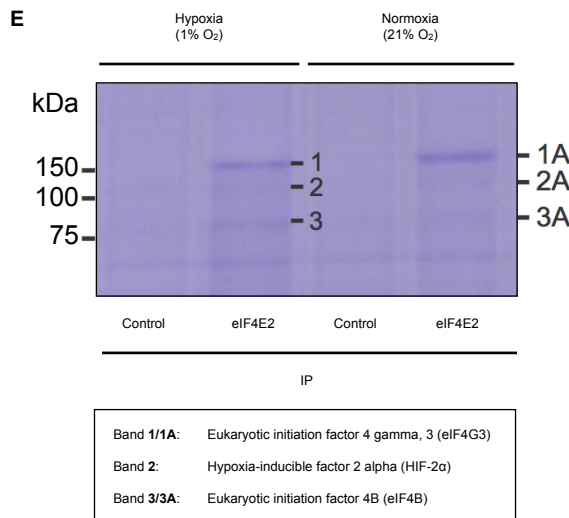
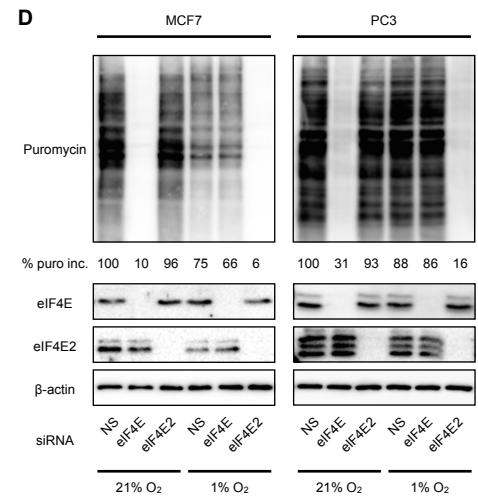
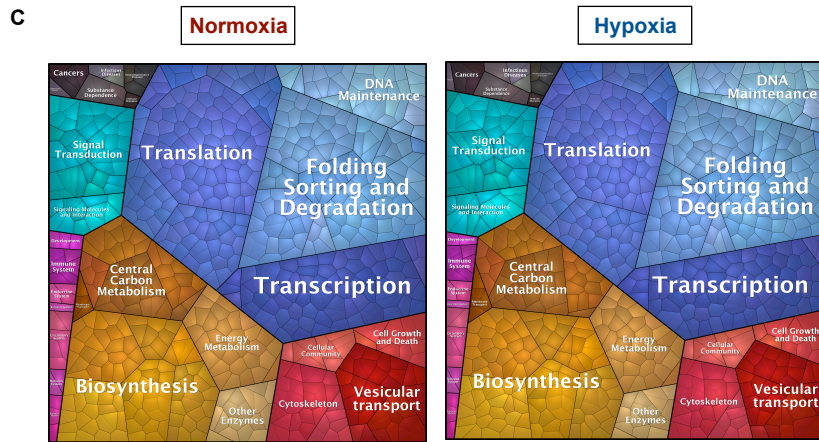
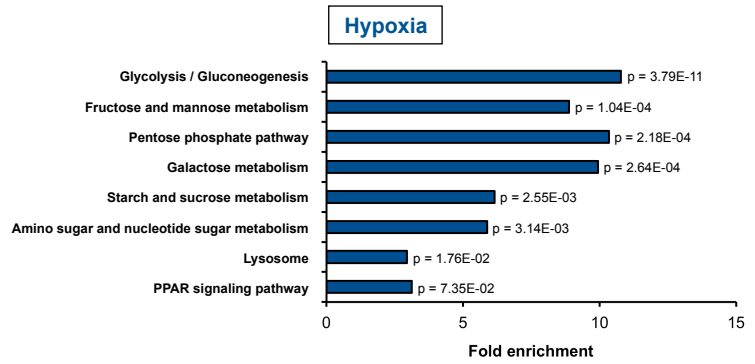
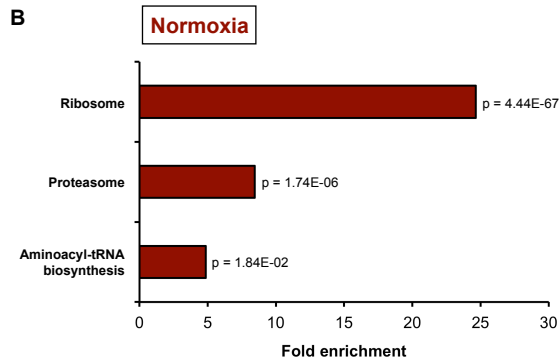
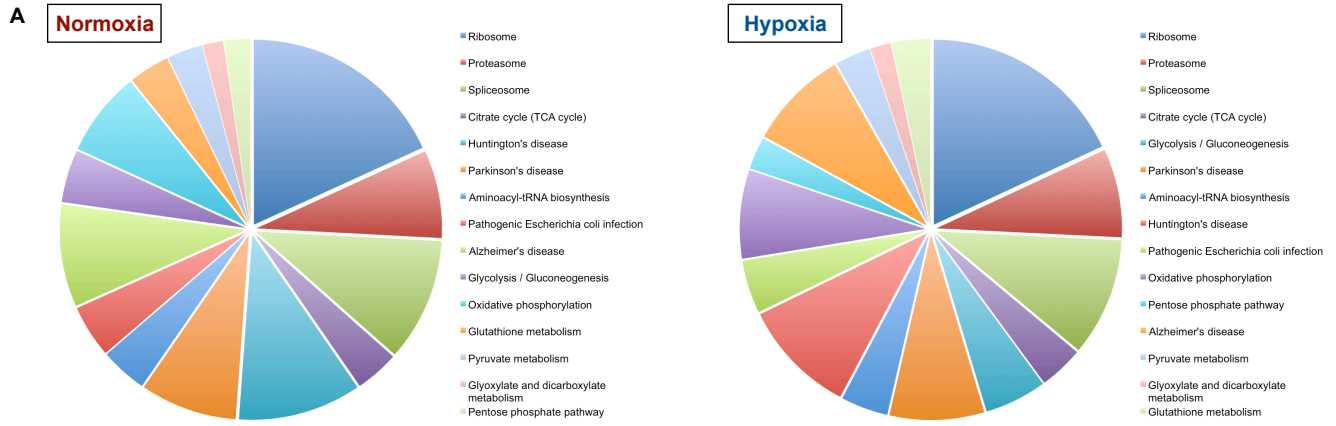


**Figure S2. Related to Figure 2.** (A) KEGG pathway enrichment analysis of pSILAC-identified proteins in normoxic (left panel) and hypoxic (right panel) U87MG using the Database for Annotation, Visualization and Integrated Discovery (DAVID) online bioinformatics resource. The top 15 enriched pathways are shown, listed in descending order of p value (clockwise direction in pie chart, top to bottom in legend). P values of listed pathways are shown in Table S1. (B) KEGG pathway enrichment analysis of proteins that are preferentially translated in normoxia (left panel) and hypoxia (right panel) by  $\geq 1.5$ -fold as identified by pSILAC in U87MG using DAVID. P values for each pathway are listed next to the corresponding bar, as well as in Table S1. (C) Visualization of KEGG pathway analysis of the pSILAC-identified proteins in normoxic (left panel) and hypoxic (right panel) U87MG using the Proteomaps quantitative visualization tool. (D) Global translation rates in normoxic and hypoxic MCF7 and PC3 transiently transfected with eIF4E-specific, eIF4E2-specific, or non-silencing (NS) control siRNA were measured using puromycin incorporation. Loading was performed on an equal cell basis. % puro inc., percent puromycin incorporation. Immunoblots of eIF4E and eIF4E2 are shown.  $\beta$ -actin was used as a loading control. (E) Coomassie blue-stained gel of FLAG-eIF4E2 immunoprecipitations (IPs) in hypoxia and normoxia (top panel). Excised bands (labeled 1, 2, 3 and 1A, 2A and 3A) were analyzed by mass spectrometry (MS). Control FLAG IPs were performed on cells transfected with an empty FLAG-expressing vector. MS results, displaying proteins with the highest abundance in each band (bottom panel). eIF4G3 was validated by immunoblotting (Figure 2C). (F) Polysome profiles of hypoxic U87MG transiently transfected with eIF4G3-specific or NS shRNA.

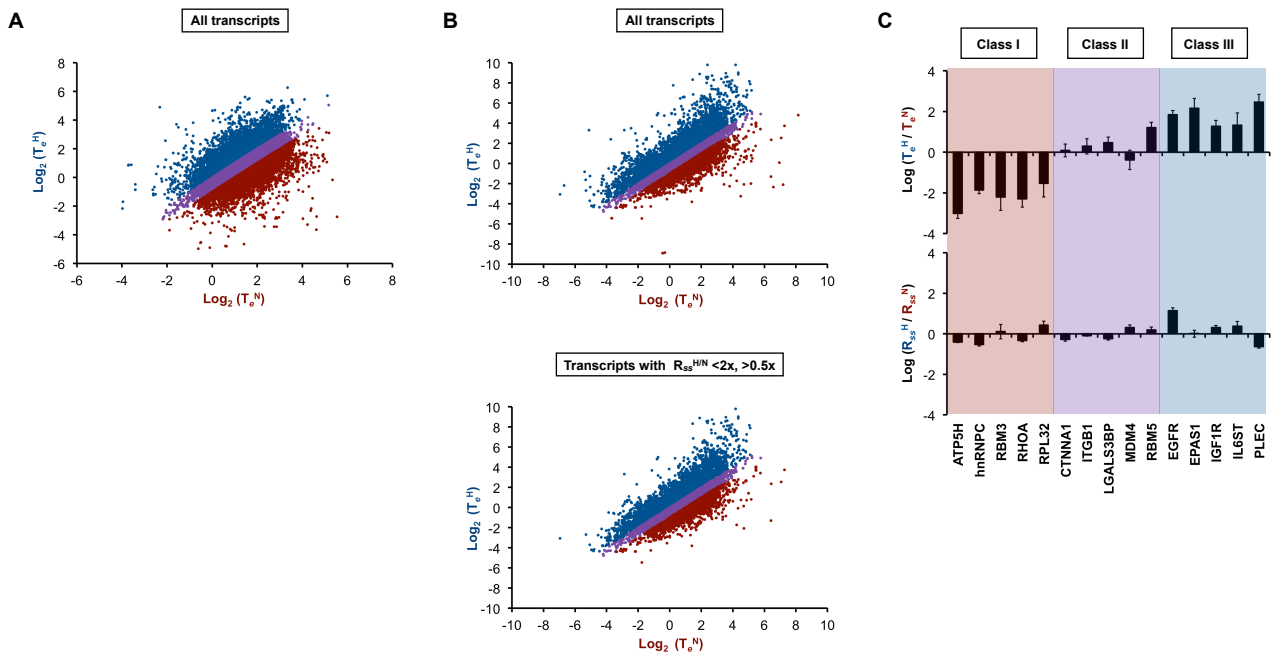


**Figure S3. Related to Figure 3.** (A) Classification of all transcripts into three major classes according to  $T_e^H/T_e^N$  ratios. Class I transcripts ( $T_e^H/T_e^N \leq 0.5$ -fold, red); Class II transcripts (purple); Class III transcripts ( $T_e^H/T_e^N \geq 1$ -fold, blue). (B) Classification of all transcripts (top panel) and transcripts with  $R_{ss}^{H/N}$  ratios between  $< 2x$  and  $> 0.5x$  (bottom panel) into three major classes according to  $T_e^H/T_e^N$  ratios based on monosome versus polysome RNA-seq analysis (Figure S1A). Class I transcripts ( $T_e^H/T_e^N \leq 0.5$ -fold, red); Class II transcripts (purple); Class III transcripts ( $T_e^H/T_e^N \geq 1$ -fold, blue). (C) qRT-PCR validation of  $T_e$  (top panel) and  $R_{ss}$  (bottom panel) changes for each class as defined in Figure 3A. Five representative candidates were chosen from each class.

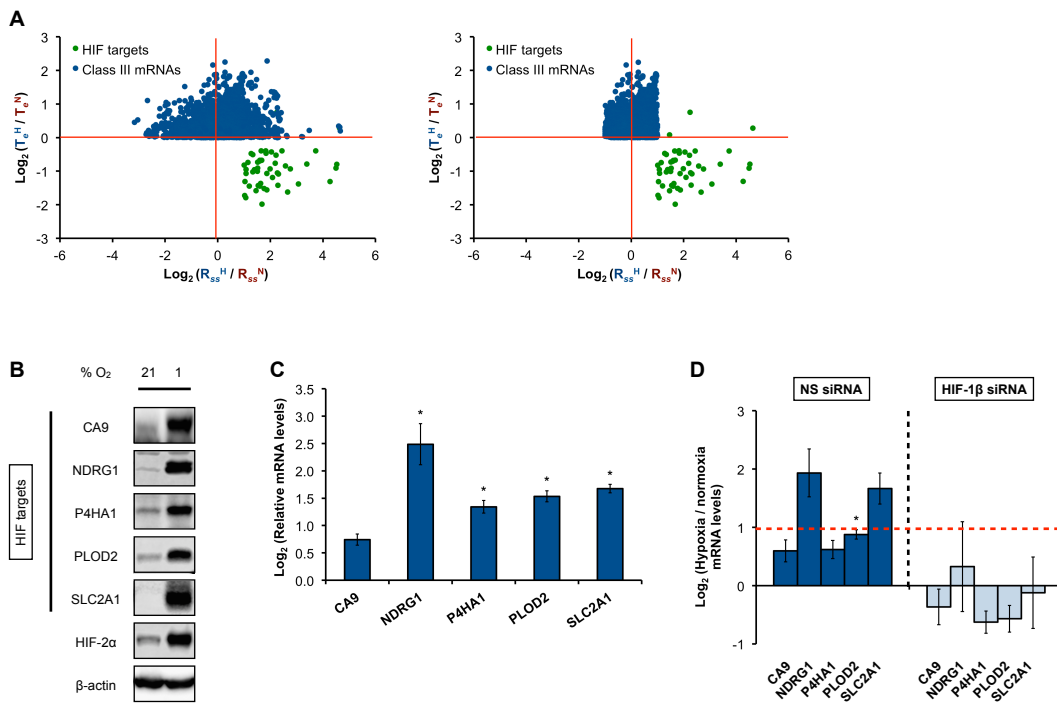


**Figure S4. Related to Figure 4.** (A) Plots of change in  $R_{ss}$  against change in  $T_e$  for 50 HIF target mRNAs (green) in hypoxic versus normoxic U87MG. All Class III members (blue) (left panel) and all Class III members with an  $R_{ss} < 2$  and  $> 0.5$  (right panel) are shown for comparison purposes. (B) Immunoblots of hypoxia-inducible, HIF target proteins in normoxic and hypoxic U87MG. HIF-2 $\alpha$  was used as a positive control for hypoxic treatment.  $\beta$ -actin was used as a loading control. (C) Corresponding hypoxic induction (hypoxia / normoxia) of steady-state mRNA levels of HIF target proteins measured in (B). \* denotes statistical significance ( $p < 0.05$ ) compared to normoxia. (D) Corresponding 4 hr hypoxia / normoxia steady-state mRNA levels of proteins measured in Figure 4C. \* denotes statistical significance ( $p < 0.05$ ) compared to 0 hr hypoxia.

## Supplemental Experimental Procedures

**Cell culture and reagents.** MCF7 human breast cancer and PC3 human prostate cancer cell lines were obtained from the American Type Culture Collection and propagated as suggested. Cells were maintained at 37 °C in a 5% CO<sub>2</sub>, humidified incubator. Cells were subjected to hypoxia (1% O<sub>2</sub>, 24 hr unless otherwise stated) at 37 °C in a 5% CO<sub>2</sub>, N<sub>2</sub>-balanced, humidified H35 HypOxystation (HypOxygen).

**Polysome fractionation and RNA isolation.** Polysome fractionations were performed essentially as previously described (Franovic et al., 2007). Briefly, cells were grown in 15 cm tissue culture plates. 100 mg/ml of cycloheximide (Amresco) were added for 10 min to cells before harvest. Cells were washed once with phosphate-buffered saline (PBS) containing 10 mg/ml of cycloheximide, and then centrifuged at 200 g, 4 °C for 10 min to pellet cells. Cells were then lysed in RNA lysis buffer (15 mM Tris-HCl (pH 7.4)/15 mM MgCl<sub>2</sub>/0.3 M NaCl/1 % Triton X-100/0.1 mg/ml cycloheximide/100 units/ml RNaseOUT). Lysates were centrifuged at 5,000 rpm, 4 °C for 5 min on a tabletop centrifuge to pellet nuclei. The supernatant was centrifuged again at 14,000 rpm, 4 °C for 5 min to pellet cell debris. Samples were then loaded onto a 10%-50% sucrose gradient based on equal cell number, and subjected to ultra-centrifugation at 39,000 rpm, 4 °C for 90 min in a SW-41-Ti rotor (Beckman Coulter), using slow deceleration. Samples were then fractionated using an automated fractionator (Brandel) into 10 equal fractions while continuously monitoring the absorbance at 254 nm. Total RNA were isolated from individual fractions by standard phenol/chloroform extraction and ethanol precipitation following proteinase K treatment. Non-coding/untranslated RNA classes (e.g. microRNAs and long non-coding RNAs), which sediment in the sub-ribosome fraction, were excluded from analysis (Dresios et al., 2005).

**RNA sequencing.** Equal volumes of individual fractions from four independent experiments were pooled to yield the monosome/oligosome (M/O; fractions 2-6) sample and the polysome (P; fractions 7-10) sample. Total RNA was processed for library construction by Cofactor Genomics (St. Louis, MO, USA) according to the following procedure: RNA was amplified using the Ovation RNA-Seq V2 amplification system (NuGEN). Double-stranded cDNA was sheared to the desired size using the Covaris S2 (Covaris). Indexed adaptors were ligated to sample DNA, and the adaptor-ligated DNA was then size-selected on a 2% SizeSelect E-Gel (Invitrogen) and amplified by PCR. Library quality was assessed by measuring nanomolar concentration and the fragment size in base pairs. Libraries were sequenced on an Illumina NextSeq 500 system (Illumina), according to the manufacturer's protocols. Raw data processing and visualization were performed by Cofactor Genomics (St. Louis, MO). Raw sequence data in FASTQ format were assessed for quality (FastQC) and ribosomal RNA content. NovoAlign v2.08 (Novocraft) was used to align reads to the reference transcriptome (a de-duplicated version of the hg19 UCSC knownGene database) and genome (hg19/GRCh37) databases. NovoAlign parameters were set to allow multiple alignments to the transcriptome set to allow for isoforms, but only unique alignments to the genome. The genome alignment loci from all samples were combined and clustered to generate genomic loci ("patches") with contiguous read coverage. Patches overlapping reference genome annotation loci were labelled as such. For each transcript or patch, the mean coverage (number of bases of read sequence aligned to the transcript or patch divided by the length of the transcript or patch) was calculated for each sample and was then further normalized by multiplying each mean coverage by the mean number of aligned reads per sample divided by the number of aligned reads for that sample. This normalized expression data was the basis for the expression values used in expression comparison and statistics generation.

Equal volumes of individual fractions from four independent experiments were pooled to yield the monosome (M; fractions 2-3) sample and the polysome (P; fractions 7-10) sample. Total RNA was

processed for library construction by the Donnelly Sequencing Centre, University of Toronto (Toronto, Ontario, Canada): Double-stranded cDNA libraries were generated from total sample RNA using the TotalScript™ RNA-Seq kit (Epicentre, Illumina), with oligo-dT priming. Libraries were sequenced on a HiSeq 2500 system, according to the manufacturer's protocols. Raw data processing and visualization were performed by Cofactor Genomics (St. Louis, MO), as described above.

**Pulse-SILAC and mass spectrometry.** Cells were maintained in “light” (R<sub>0</sub>K<sub>0</sub>) media under standard cell culture conditions at 21% O<sub>2</sub>, following which they were subjected to pre-treatment with 1% O<sub>2</sub> or 21% O<sub>2</sub> for 6 hr. Light media was then removed and cells were washed once with PBS to maximize removal of residual light media. “Heavy” (R<sub>10</sub>K<sub>8</sub>) media was then added to the cells, which were left to grow at 1% O<sub>2</sub> or 21% O<sub>2</sub> for 24 hr. Following 24 hr of labeling with heavy media, total cellular protein were harvested using a urea lysis buffer (9 M Urea, 20 mM HEPES at pH 8.0). Lysates were centrifuged at 20,000 g for 15 min at 4 °C, and the supernatant were subjected to in-solution digestion followed by liquid chromatography tandem mass spectrometry analysis (LC-MS/MS). Samples were analyzed on a linear ion trap-Orbitrap hybrid analyzer (Orbitrap Elite, Thermo Fisher Scientific) outfitted with a nanospray source and EASY-nLC split-free nano-LC system (Thermo Fisher Scientific). Lyophilized peptide mixtures were dissolved in 0.1% formic acid and loaded onto a 75µm x 50cm PepMax RSLC EASY-Spray column filled with 2 µM C18 beads (Thermo Fisher) at a pressure of 800 BAR. Peptides were eluted over 240 min at a rate of 250 nl/min using a 0 to 35% acetonitrile gradient in 0.1% formic acid. Peptides were introduced by nano electrospray into an Orbitrap Elite hybrid mass spectrometer (Thermo Fisher Scientific). The instrument method consisted of one MS full scan (400–1500 m/z) in the Orbitrap mass analyzer, an automatic gain control target of 500,000 with a maximum ion injection of 200 ms, one microscan, and a resolution of 120,000. Ten data-dependent MS/MS scans were performed in the linear ion trap using the ten most intense ions at 35% normalized collision energy. The MS and MS/MS scans were obtained in parallel fashion. In MS/MS mode automatic gain control targets were 10,000 with a maximum ion injection time of 100 ms. A minimum ion intensity of 1000 was required to trigger an MS/MS spectrum. Dynamic exclusion was applied using a maximum exclusion list of 500 with one repeat count with a repeat duration of 15 s and exclusion duration of 45 s. Alternatively, cells were sequentially extracted into Digitonin-soluble, Triton-soluble, and Triton-insoluble fractions. These fractions were separated by size on a 4 – 20% Tris-Glycine (TGX) gel (Biorad), following which each lane was cut into 8 equal-sized bands. Gel bands were then subjected to in-gel digestion followed by LC-MS/MS on an LTQ-Orbitrap XL hybrid ion trap mass spectrometer (Thermo Fisher Scientific). Raw data generated by LC-MS/MS of both experiments (peaklists generated by Xcalibur 2.2) were combined and analyzed using Xcalibur (Thermo Fisher Scientific) for ion current analysis, and were searched against the international protein index human database, downloaded from <http://www.ebi.ac.uk/IPI/IPIhelp.html> (downloaded May 13 2014). Database searching was done by using SEQUEST version 1.3.0.339 (through Proteome Discoverer, Thermo Fisher Scientific). SEQUEST search data was then imported into Scaffold (Proteome Software) and X!Tandem database searching was performed on import. Databases were searched with a parent ion tolerance of 10.0 PPM, and a fragment mass tolerance of 0.6Da. Deamidation of asparagine and glutamine, label:13C(6)15N(2) of lysine, label:13C(6)15N(4) of arginine and oxidation of methionine were specified as variable modifications. Proteins were annotated with GO terms from gene\_association.goa\_human (downloaded Nov 4, 2014) (Ashburner et al., 2000). Scaffold Q+ (version Scaffold\_4.4.3, Proteome Software) was used to quantitate SILAC Label Based Quantitation peptide and protein identifications. Peptide identifications were accepted if they could be established at greater than 95.0% probability by the Scaffold Local FDR algorithm. Protein identifications were accepted if they could be established at greater than 95.0% probability and contained at least 2 identified peptides. Protein probabilities were assigned by the Protein Prophet algorithm (Nesvizhskii et al., 2003). Proteins that contained similar peptides and could not be differentiated based on MS/MS analysis



alone were grouped to satisfy the principles of parsimony. Acquired intensities in the experiment were globally normalized across all acquisition runs. Individual quantitative samples were normalized within each acquisition run. Intensities for each peptide identification were normalized within the assigned protein. The reference channels were normalized to produce a 1:1 fold change. All normalization calculations were performed using averages to multiplicatively normalize data. Scaffold Q+ was used to determine the Log<sub>2</sub> of the normalized heavy label intensities. Both normoxia and hypoxia light channels were considered references, while the heavy channels were compared against each other.

**KEGG analysis and visualization.** Proteins identified from the pulse-SILAC analysis were subjected to KEGG analysis using DAVID (<https://david.ncifcrf.gov>) (Huang da et al., 2009), and visualized using the Proteomaps software (<http://www.proteomaps.net>) (Liebermeister et al., 2014).

**Immunofluorescence.** Cells were treated with 5-fluorouridine (5-FU) (Sigma-Aldrich) at a final concentration of 1 mM for 1 hr. Cells were then fixed with 4% formaldehyde, permeabilized with 0.5% Triton X-100, and detected using an anti-bromodeoxyuridine antibody (Sigma-Aldrich) and a Alexa Fluor 488-conjugated secondary antibody (ThermoFisher).

**Immunoprecipitation.** Immunoprecipitations were performed as previously described (Franovic et al., 2007).

**Immunoblot.** Immunoblots were performed using standard techniques. Primary monoclonal antibodies were used to detect  $\beta$ -actin (Thermo Fisher Scientific), BNIP3 (Abcam), EGFR (Thermo Fisher Scientific), eIF4E (Santa Cruz Biotechnology), HIF-1 $\beta$  (BD Transduction Laboratories), LGALS3 (Abcam), MDM4 (Abcam), NDRG1 (Novus Biologicals), puromycin (Kerafast), and RBM3 (Abcam). Primary polyclonal antibodies were used to detect BNIP3L (Abcam), eIF4B (Cell Signaling), eIF4E2 (Genetex), eIF4G1 (Novus Biologicals), eIF4G3 (Genetex), GAPDH (Abcam), HIF-2 $\alpha$  (Novus Biologicals), LDHA (Abcam), MIF (Abcam), P4HA1 (Novus Biologicals), PLOD2 (Novus Biologicals), RBM5 (Novus Biologicals), RPL32 (Abcam), and SLC2A1 (Novus Biologicals). HRP-conjugated anti-mouse (Life Technologies) and anti-rabbit (Life Technologies) secondary antibodies were used. Signals were detected by chemiluminescence (Millipore), and analyzed in ImageJ (NIH).

**Quantitative reverse transcription-polymerase chain reaction (qRT-PCR).** First-strand cDNA synthesis was performed using the high-capacity cDNA reverse transcription kit (Life Technologies), according to the manufacturer's protocol. qRT-PCR was performed using the iTaq universal SYBR green supermix (Biorad) and a CFX96 Touch real-time PCR detection system (Biorad). All primer sequences are available upon request. Relative fold changes in expression were calculated using the comparative Ct ( $\Delta\Delta$ Ct) method.

**Statistical analysis.** Cohen's kappa coefficient is a robust measure of concordance between two categorical readouts that takes into account the agreement occurring by chance. Individual values of each parameter (i.e.  $R_{ss}$ ,  $T_e$ , and pSILAC) were categorized as "positive" (> mean of all data points) or "negative" (< mean of all data points) in hypoxic versus normoxic cells. Calculation of Cohen's kappa was then performed to analyze the degree of concordance between  $R_{ss}$ ,  $T_e$ , and pSILAC in a pairwise manner.

## Supplemental References

Ashburner, M., Ball, C.A., Blake, J.A., Botstein, D., Butler, H., Cherry, J.M., Davis, A.P., Dolinski, K., Dwight, S.S., Eppig, J.T., *et al.* (2000). Gene ontology: tool for the unification of biology. The Gene Ontology Consortium. *Nature genetics* 25, 25-29.

Dresios, J., Aschrafi, A., Owens, G.C., Vanderklish, P.W., Edelman, G.M., and Mauro, V.P. (2005). Cold stress-induced protein Rbm3 binds 60S ribosomal subunits, alters microRNA levels, and enhances global protein synthesis. *Proceedings of the National Academy of Sciences of the United States of America* 102, 1865-1870.

Huang da, W., Sherman, B.T., and Lempicki, R.A. (2009). Systematic and integrative analysis of large gene lists using DAVID bioinformatics resources. *Nat Protoc* 4, 44-57.

Liebermeister, W., Noor, E., Flamholz, A., Davidi, D., Bernhardt, J., and Milo, R. (2014). Visual account of protein investment in cellular functions. *Proceedings of the National Academy of Sciences of the United States of America* 111, 8488-8493.

Nesvizhskii, A.I., Keller, A., Kolker, E., and Aebersold, R. (2003). A statistical model for identifying proteins by tandem mass spectrometry. *Analytical chemistry* 75, 4646-4658.